Am J Nucl Med Mol Imaging 2014;4(4):365-384
www.ajnmmi.us /ISSN:2160-8407/ajnmmi0000557

Review Article

PET radiopharmaceuticals for imaging of tumor hypoxia: *a review of the evidence*

Egesta Lopci[1,2], Ilaria Grassi[1], Arturo Chiti[2], Cristina Nanni[1], Gianfranco Cicoria[3], Luca Toschi[4], Cristina Fonti[1], Filippo Lodi[1], Sandro Mattioli[5], Stefano Fanti[1]

[1]Department of Nuclear Medicine, University Hospital S. Orsola-Malpighi, Bologna, Italy; [2]Department of Nuclear Medicine, Humanitas Clinical and Research Center, Rozzano, Italy; [3]Department of Medical Physics, University Hospital S. Orsola-Malpighi, Bologna, Italy; [4]Department of Medical Oncology, Humanitas Clinical and Research Center, Rozzano, Italy; [5]Division of Thoracic Surgery, University Hospital S. Orsola-Malpighi, Bologna, Italy

Received April 17, 2014; Accepted April 28, 2014; Epub June 7, 2014; Published June 15, 2014

Abstract: Hypoxia is a pathological condition arising in living tissues when oxygen supply does not adequately cover the cellular metabolic demand. Detection of this phenomenon in tumors is of the utmost clinical relevance because tumor aggressiveness, metastatic spread, failure to achieve tumor control, increased rate of recurrence, and ultimate poor outcome are all associated with hypoxia. Consequently, in recent decades there has been increasing interest in developing methods for measurement of oxygen levels in tumors. Among the image-based modalities for hypoxia assessment, positron emission tomography (PET) is one of the most extensively investigated based on the various advantages it offers, i.e., broad range of radiopharmaceuticals, good intrinsic resolution, three-dimensional tumor representation, possibility of semiquantification/quantification of the amount of hypoxic tumor burden, overall patient friendliness, and ease of repetition. Compared with the other non-invasive techniques, the biggest advantage of PET imaging is that it offers the highest specificity for detection of hypoxic tissue. Starting with the 2-nitroimidazole family of compounds in the early 1980s, a great number of PET tracers have been developed for the identification of hypoxia in living tissue and solid tumors. This paper provides an overview of the principal PET tracers applied in cancer imaging of hypoxia and discusses in detail their advantages and pitfalls.

Keywords: Hypoxia, tumor imaging, PET, ^{18}F-FDG, ^{18}F-FMISO, ^{18}F-FAZA, ^{64}Cu-ATSM

Introduction

Hypoxia is a pathological condition arising in living tissue when the oxygen supply does not adequately cover the cellular metabolic demand. This phenomenon is also present in the vast majority of solid tumors and has been associated with a tendency toward poor prognosis [1]. The first to demonstrate the presence of hypoxia in human tumors were Tomlinson and Gray in the early 1960s [2]. So far we have evidence that up to 60% of locally advanced solid tumors are characterized by areas of reduced (hypoxia) or almost absent oxygen supply (anoxia) [3]. Detection of this phenomenon in tumors is of the utmost clinical relevance, because tumor aggressiveness, metastatic spread, failure to achieve tumor control, increased rate of recurrence, and ultimate poor outcome are all associated with hypoxia [4].

Onset of hypoxia in tumors is often the result of abnormal perfusion, which is typical of tumor-related neoangiogenesis and predominantly causes a transient hypoxia (acute hypoxia). In other cases hypoxia is caused by insufficient oxygen diffusion due to increased distance between the involved tissue and the blood supply (chronic hypoxia) or, to be more specific, a distance exceeding 100 μm from the nearest blood vessel, this being the diffusion distance of soluble oxygen [2]. Another mechanism of hypoxia induction is altered oxygen transport, such as occurs in disease- and/or treatment-related anemia [1, 3, 5-7].

The hypoxia epiphenomenon is translated into a downstream cascade of cellular adaptation mechanisms and is associated with various changes in gene expression, mostly mediated by the hypoxia-inducible factors 1 and 2 (HIF-1α

and HIF-2) [5]. As reported by Post and Van Meir, the level of HIF gene activation is a function of oxygen concentration and increases exponentially when O_2 levels fall below 5% [8]. In general the median pressure of oxygen (pO_2) at which living tissues experience hypoxia is cited as around 8-10 mmHg [9, 10]. At these oxygen levels, HIFs will trigger activation of genes involved in glycolysis, cell proliferation, cell survival, angiogenesis, and metastatic invasion [5, 11]. This pattern of gene expression alters the malignant potential of tumors, following which cancer cells can become resistant to radiation treatment and chemotherapy [12, 13].

Consequently, in recent decades there has been increasing interest in developing methods for measurement of the levels of oxygen in tumors. These methods can be invasive, such as the polarographic O_2 sensor (Eppendorf GmbH, Hamburg, Germany), or non-invasive, mainly based on imaging techniques [12]. Imaging modalities are undoubtedly more appealing for the assessment of tumor hypoxia because they guarantee all-encompassing visualization of the neoplastic tissue and can identify the phenomenon even at sites inaccessible to invasive procedures. Among the many techniques now available are optical-based methods, magnetic resonance imaging (MRI), and nuclear medicine techniques [14, 15]. Some of their principal characteristics and limitations are summarized in **Table 1**, although an in-depth understanding of the value of each modality would require a more extensive report, which is beyond the scope of this review [14-18].

Among the image-based modalities for hypoxia assessment, positron emission tomography (PET) is one of the most extensively investigated based on the various advantages it offers: (a) a broad assortment of radiopharmaceuticals; (b) good intrinsic resolution (5 mm); (c) three-dimensional (3D) tumor representation; (d) possibility of semiquantification/quantification of the hypoxic tumor burden; (e) overall patient friendliness, and (f) ease of repetition [19]. Compared with the other non-invasive techniques, however, the biggest advantage of PET is that it displays the highest specificity for hypoxic tissue [20].

The object of the current paper is therefore to provide an overview of the principal PET radiopharmaceuticals applied in cancer imaging of hypoxia and to discuss in detail their advantages and pitfalls.

PET imaging of hypoxia

Starting with the 2-nitroimidazole family of compounds in the early 1980s [15, 21], a great number of PET tracers have been developed for the identification of hypoxia in living tissues and solid tumors (**Table 2**). The driving force behind this development has been the need for highly specific imaging "probes" able to overcome the inconsistent correlation between findings on other imaging modalities, including PET with ^{18}F-fluorodeoxyglucose (^{18}F-FDG), and the hypoxia levels determined in tumor tissue [3, 15, 22].

^{18}F-fluorodeoxyglucose (^{18}F-FDG)

Undoubtedly ^{18}F-FDG PET remains a cornerstone for tumor evaluation, response assessment, and disease prognostication, but it requires careful handling when trying to depict hypoxic tissue. The fact that tumor hyperglycolysis due to up-regulation of glucose transporters (GLUTs) and glycolytic enzymes can be driven by HIF-1α [22, 23] offers some justification for the use of ^{18}F-FDG as a surrogate marker of hypoxia [24]. Moreover, we know that under reduced levels of oxygen ($\downarrow pO_2$), living cells switch their metabolic pathway for ATP production to anaerobic glycolysis, also known as the Pasteur effect [25].

However, in the case of hypoxic tumor cells, a wide overlap exists between ^{18}F-FDG uptake due to aerobic glycolysis, the so-called Warburg effect [26], and anaerobic glycolysis [25, 27] (i.e., normoxic and hypoxic conditions, respectively) (**Figure 1**). The fact that HIF-1α expression can be observed also in non-hypoxic tumor regions [28, 29] suggests that other factors can indirectly influence glucose metabolism and ^{18}F-FDG uptake in those areas [22]. It therefore appears comprehensible why, in many experiments, the correlation between ^{18}F-FDG uptake and the level of tumor hypoxia has not been confirmed or conflicting results have been obtained [3, 30]. These shortcomings apply to the imaging of a variety of tumor types, including head and neck carcinoma, lung cancer, sarcomas, breast cancer, and brain tumors [22, 31-38]. For instance, in two different studies of, respectively, 24 and 36 patients

Table 1. Examples of non-invasive methods for hypoxia determination in living tissues [14-18]

Modality		Technique	Limitations
Optical-based	Phosphorescence	Infusion of water-soluble phosphor probes into the vasculature.	The measurement represents the vascular pO_2, not tissue pO_2.
	Near-infrared spectroscopy (NIRS)	Non-invasive assessment of hemoglobin (Hb) saturation.	The measurement provides information on vascular oxygenation, but not on tissue pO_2.
MRI-based	Blood oxygen level-dependent magnetic resonance imaging (BOLD MRI)	BOLD images reveal the changes in the amount of oxygen bound to hemoglobin in blood owing to deoxyhemoglobin, which is a paramagnetic substance.	The measurement provides information on changes in blood oxygenation, but not on the absolute oxygen concentration in tissue.
	^{19}F-MRI or NMR (nuclear magnetic resonance)	Perfluorocarbons (PFCs) are injected intravenously and their ^{19}F spin lattice relaxation rate (R1) varies linearly with the dissolved oxygen concentration.	The relaxation rate of ^{19}F may depend on other physiological factors present in the tissue and not only on O_2 concentration.
	Electron paramagnetic resonance imaging (EPRI)	Use of implantable paramagnetic particulates or soluble probes, intravenously injected, that physically interact with oxygen.	The molecules may predominantly distribute in the vasculature, thus biasing in part measurements of tissue oxygenation.
	Proton–electron double resonance imaging (PEDRI)	Injection of an external probe that has unpaired electrons and use of a strong EPR impulse.	The molecules may predominantly distribute in the vasculature, thus biasing in part measurements of tissue oxygenation.
	DCE-MRI (dynamic Gd-DTPA-enhanced MRI)	Injection of contrast agent and determination of vasculature perfusion/permeability.	Low specificity, because the measurement provides information on both vascular and tissue oxygenation.
Nuclear-based	Single-photon emission computed tomography (SPECT)	Injection of gamma (γ) emitting radiopharmaceuticals selective for hypoxic tissue. High specificity	Limited resolution dependent on voxel-based distribution of hypoxia.
	Positron emission tomography (PET)	Injection of positron (β+) emitting radiopharmaceuticals selective for hypoxic tissue. High specificity.	Limited resolution compared to MRI and optical methods, but superior to SPECT.

with head and neck squamous carcinoma [31, 33], direct comparison of ^{18}F-FDG uptake and hypoxia determination using a polarographic O_2 sensor documented a lack of correlation. Similarly, no correlation of glucose metabolism on ^{18}F-FDG PET and hypoxia was observed in non-small cell lung cancer (NSCLC) patients [32-34]. These data are not to be considered absolutely negative, because ^{18}F-FDG has been documented to be capable of defining more aggressive tumor types, also correlated with HIF-1α expression, in patients with gastric carcinoma [39] or tongue cancer [40], as well as in those with both the above-mentioned neoplasia, i.e., NSCLC [23, 27] and oral squamous cell carcinoma [40, 41].

In summary, the limitations on the specific application of ^{18}F-FDG for the detection of hypoxia persist, and in the case of tumor imaging it is advisable to combine this tracer with other hypoxia-avid ones in order to achieve a comprehensive assessment of the tumor characteristics [25].

Nitroimidazole family of compounds

^{18}F-fluoromisonidazole (^{18}F-FMISO)

The fluorinated nitroimidazole derivative ^{18}F-fluoromisonidazole, or ^{18}F-FMISO, is the most widely studied PET tracer for hypoxia imaging. It was first developed for this purpose in 1986 [82, 83] and since then has been extensively used for the detection of many tumor types in both the preclinical and the clinical context [3, 15]. Like the other compounds in the nitroimidazole family, this tracer is passively diffused through the cell membrane owing to its lipophilicity, and once within the intracellular environment it is reduced into R-NO_2 radicals by the nitroreductase enzyme (NTR) (**Figure 1**). This process is still reversible and when the cell is well oxygenated, the tracer is not entrapped and can freely flow back into the extracellular environment. Conversely, in the presence of reduced levels of oxygen (pO_2 <10 mmHg) the process of ^{18}F-FMISO reduction continues slowly; the consequence is the progressive production of R-NHOH compounds that bind covalently to intracellular molecules, and ultimately entrapment of the tracer within the cell [59, 84, 85].

The amount of ^{18}F-FMISO uptake is therefore influenced by the O_2 level in tumor tissue, as is confirmed by the good correlation observed between tracer uptake and pO_2 polarography [32, 33] or immunohistochemical determination of hypoxia [86, 87]. However, the time line of the above-mentioned processes is rather long for an ^{18}F-fluorine labeled tracer ($T_{1/2}$ 109

Table 2. Principal radiopharmaceuticals applied in PET imaging of tumor hypoxia

Uptake mechanism	Tracer	Tumors imaged	Benefits	Limitations
Pasteur effect (anaerobic glycolysis) [25]	^{18}F-FDG (^{18}F-fluorodeoxyglucose)	NSCLC [23, 27, 32, 37] Head and neck tumors [31] Oral squamous cell carcinoma [40, 41] Gastric cancer [39]	Good correlation with tumor aggressiveness and prognosis Easily reproducible and broad availability	Overlap between uptake in normoxic (Warburg effect) [26] and hypoxia tumor tissue
Nitroimidazole-like uptake: reduction into RNO2 radicals and RNHOH compounds in hypoxic conditions. Then covalent binding to macromolecules [21, 59]	^{18}F-MISO (^{18}F-fluoromisonidazole)	Head and neck tumors [35, 42-45] Locally advanced HNSCC [35, 46] Glioblastoma multiforme (GBM) [37, 47, 48] Breast cancer [49] NSCLC [32, 33, 50] Renal cell carcinoma [51]	Broadest evidence of value as a hypoxia tracer. Good correlation with immunohistochemistry and prognosis in most cases. Good availability	Lack of correlation in all tumors Low tumor-to-background ratio Variable reproducibility
	^{18}F-FAZA (^{18}F-fluoroazomycin-arabinozide)	Head and neck tumors [52, 53] Cervical cancer [54] Prostate cancer [55] NSCLC [56, 57] Rectal cancer [58]	Good correlation with immunohistochemistry and prognosis in most cases. Faster diffusion and clearance with slightly higher tumor-to-background ratio than ^{18}F-MISO.	More limited evidence compared to ^{18}F-MISO.
	^{18}F-FETNIM (^{18}F-fluoroerythronitroimidazole)	NSCLC [60] Esophageal cancer [61]	Promising tracer with possible correlation with outcome. Slightly higher tumor-to-background ratio than ^{18}F-MISO.	Limited evidence compared to ^{18}F-MISO.
	^{18}F-EF5 (^{18}F-2-nitroimidazol-pentafluoropropyl acetamide)	Brain tumors [62] Soft tissue sarcoma [63] Head and neck tumors [64]	Promising tracer with possible correlation with outcome	Limited evidence.
	^{18}F-EF3 (^{18}F-2-nitroimidazol- trifluoropropyl acetamide)	Rats bearing syngeneic rhabdomyosarcoma tumours [65] Head and neck tumors [66]	Promising tracer.	Very limited evidence, mostly preclinical.
	^{18}F-FETA (^{18}F-fluoroetanidazole)	Mice bearing MCF-7, RIF-1, EMT6, HT1080/26.6, and HT1080/1-3C xenografts [67, 68]	Promising tracer with better biodistribution than ^{18}F-MISO.	Preclinical evidence
	^{124}I-IAZG (^{124}I-iodoazomycin galactopyranoside)	Hepatocellular carcinoma [69]	Promising tracer	Preclinical evidence
	^{68}Ga-labeled nitroimidazole analogs (^{68}Ga-NOTA-nitroimidazole, ^{68}Ga-DOTA-nitroimidazole, ^{68}Ga-SCN-NOTA-nitroimidazole)	Tumor xenografted mice [70, 71]	Promising tracer	Preclinical evidence
Reduction of Cu(II)-ATSM complex into Cu(I)-ATSM and dissociation of Cu(I) in hypoxic conditions: then Cu(I) nuclide binding to intracellular proteins [77]	^{60,61,62,64}Cu-ATSM (^{60,61,62,64}Cu-diacetyl-bis(*N*4-methylthiosemicarbazone)	NSCLC [34] Head and neck tumors [72, 73] Cervical cancer [74, 75] Rectal cancer [76] Brain tumors [78]	Good correlation with immunohistochemistry and prognosis. Early uptake of the tracer with high tumor-to-background ratio. Possibility for late acquisition with ^{64}Cu-ATSM. Possibility for radionuclide therapy with ^{64}Cu-ATSM.	Evidence more limited compared to ^{18}F-MISO. Less clear mechanism of uptake in tumor hypoxia compared to nitroimidazole-like compounds.
Recognizes carbonic anhydrase IX (CA IX) [80]	^{124}I-cG250 (^{124}I-chimeric mAb G250)	Renal cell carcinoma [79]	Promising tracer	Preclinical evidence
	^{89}Zr-cG250-F(ab′)$_2$ (^{89}Zr-chimeric G250 F(ab′)$_2$)	Head and neck tumors [81]	Promising tracer	Preclinical evidence

Abbreviations: HNSCC, head and neck squamous cell carcinoma; NSCLC, non-small cell lung cancer.

min), because selective retention of ^{18}F-FMISO in hypoxic tissue requires an uptake period of around 2-4 h after intravenous injection [11, 45, 88]. In addition, despite this uptake period, tracer accumulation is still low, as documented by the low tumor-to-plasma or tumor-to-muscle ratio of 1.2-1.4, used as the optimal cut-off for definition of hypoxia [15, 45]. These aspects represent the main drawbacks of ^{18}F-FMISO, and may limit the applicability of the tracer in clinical practice. To overcome the problem, a dynamic approach has been tested by Thorwarth et al. [89, 90], in which a kinetic analysis is used to separate the component associated with hypoxia-specific tracer binding from that related to unbound tracer. This kinetic approach is, however, cumbersome and still restricted by the resolution limit of the technology itself.

Hypoxia imaging with ^{18}F-FMISO has been investigated in numerous solid tumors, including gliomas [38, 47, 48, 91], head and neck carcinoma [42-46], NSCLC [33, 50], breast tumors [49], and renal carcinoma [51] (**Table 2**). In patients with brain tumors, for instance, Hirata et al. [48] supported a role for ^{18}F-FMISO PET in differentiating glioblastoma multiforme (GBM) from other less malignant gliomas based on the level of tumor hypoxia. Moreover, Swanson et al. [92] reported a good correlation between the hypoxic volume determined by ^{18}F-FMISO and the MRI-defined tumor burden, with particular interest on disrupted vasculature on gadolinium-enhanced T1-weighted sequences (T1Gd). Their data confirm that the angiogenic process is stimulated by hypoxia in GBM and indirectly anticipate the more recently reported association between tumor aggressiveness visualized on ^{11}C-methionine imaging, disrupted blood–brain barrier vasculature on contrast-enhanced-MRI, and hypoxia depicted with ^{18}F-FMISO [93].

Additionally, PET imaging with ^{18}F-FMISO has been shown to discriminate prognosis in GBM For example, Spence et al. [47] studied 22 GBM patients before biopsy or between resection and radiation therapy (RT) and observed both the volume and the intensity of hypoxia as determined by ^{18}F-FMISO before therapy to be strongly correlated with time to progression and survival.

Similarly, in patients with head and neck tumors, Rajendran et al. [43] documented a prognostic role for pretherapy ^{18}F-FMISO uptake with respect to overall survival, with hypoxic volume and nodal involvement also being predictive factors. Rischin et al. [94] demonstrated that in patients receiving-non-tirapazamine-containing chemoradiotherapy for stage III or IV head and neck tumors, hypoxia on FMISO PET was associated with a higher rate of locoregional failure. The introduction of kinetic analysis of ^{18}F-FMISO, as reported by Eschmann et al. [42], could also predict higher risk of relapse.

In 20 postmenopausal women with stage II-IV breast cancer, Cheng et al. [49] analyzed the role of ^{18}F-FMISO PET before and after endocrine therapy with letrozole. Tracer uptake was detected at 2 and 4 h after injection and tumor-to-background ratio was correlated to treatment outcome after 3 months. The authors observed a positive correlation between baseline ^{18}F-FMISO uptake and response to therapy ($p < 0.0001$) and could define a tumor-to-background ratio at 4 h of ≥ 1.2 as the optimal cut-off point, allowing the prediction of 88% (15/17) of cases of progressive disease. No correlation, however, was found between ^{18}F-FMISO uptake and HIF-1α expression at immunohistochemistry.

An important application for hypoxia imaging is undoubtedly RT planning. It is well known that the pretreatment oxygenation in cancer tissue influences response to treatment, because treatment effectiveness is strictly related to the amount of free oxygen radicals. Consequently the radiation dose necessary to achieve the same therapeutic effect is much higher for hypoxic tumors [88]. ^{18}F-FMISO has therefore been investigated in this context. Starting with their feasibility study, Lee et al [45] reported the use of ^{18}F-FMISO PET to increase the dose to hypoxic regions in head and neck carcinoma. In the same clinical setting, they tried to determine the reproducibility of the PET scan at two different time points prior to RT [95] and to assess the influence on dose-painting at intensity-modulated radiotherapy (IMRT) [96]. On the basis of these studies they concluded that changes in the spatial distribution of tumor hypoxia, as detected by serial FMISO PET, compromised the coverage of hypoxic tumor volumes achievable by dose-painting IMRT [96]. However, even when such changes occurred, dose-painting always increased the equivalent uniform dose of the hypoxic areas. In rectal

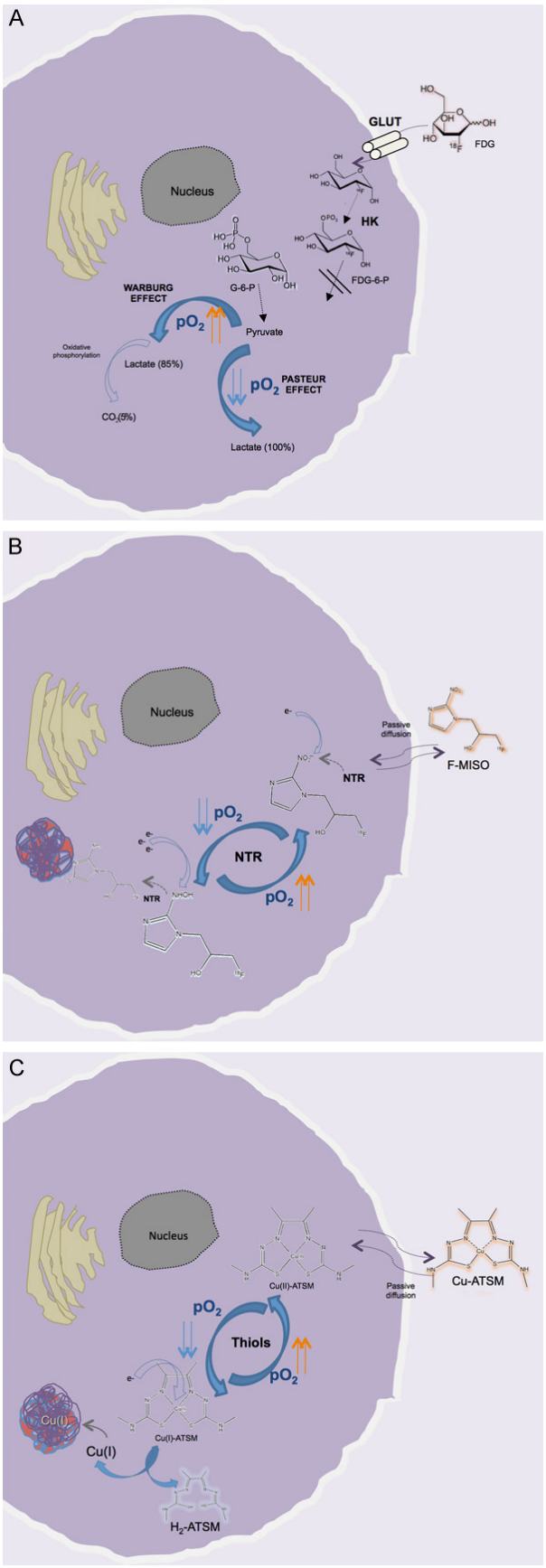

Figure 1. Overview of the uptake and retention mechanisms of FDG (A), F-MISO (B), and Cu-ATSM (C) in living cells under hypoxic conditions. For FDG there is a wide overlap between the cellular uptake in normoxic (Warburg effect) and hypoxic conditions (Pasteur effect). For the other two tracers, after passive diffusion through the membrane, the radiopharmaceutical is retained according to the oxygen tension (pO_2) present in the intracellular environment: in the presence of reduced pO_2, F-MISO undergoes progressive reduction by the nitroreductase enzyme (NTR); also, Cu(II)-ATSM nuclide is reduced to copper (I) by the intracellular thiols, making the Cu-ATSM complex less stable. Both processes are reversible in the presence of sufficient O_2, and the molecules (F-MISO and Cu (II)-ATSM) are free to leave the cell. Conversely, in hypoxic conditions the Cu(I)-ATSM complex is progressively dissociated, with the formation of H_2-ATSM and free Cu(I), which is very rapidly incorporated into intracellular proteins. In contrast, the reduced F-MISO is covalently bound to the intracellular proteins [59, 84, 122, 128]. *GLUT*, glucose transporter; *HK*, hexokinase; *G-6-P*, glucose-6-phosphate).

cancer, the use of ^{18}F-FMISO PET for target definition prior to RT [97] appears less reliable due to non-specific tracer uptake in normoxic tissue and diffusion through the bowel wall.

High reproducibility of tumor hypoxia evaluated by ^{18}F-FMISO PET was recently reported by Okamoto et al. [98] in 11 patients with untreated head and neck cancer who were investigated twice with ^{18}F-FMISO PET at an interval of 48 h. In this cohort the 4-h tracer uptake parameters (SUV_{max}, tumor-to-background, and tumor-to-muscle ratio) showed no significant difference between the scans and, except in one case, the location of the SUV_{max} peaks, although different in PET1 and PET2, were within the full-width at half-maximum of the PET/CT scanner.

In a prospective study by Tachibana et al. [99] a limited cohort of ten patients was studied before and during fractionated RT with ^{18}F-FMISO PET/CT in order to determine the intratumoral hypoxic areas and their reoxygenation. The study revealed a high percentage of tumor reoxygenation (8/10) during RT, suggesting that dose escalation to the hypoxic areas on the initial PET/CT scan might be inappropriate. However, the authors suggested that if frequent imaging with ^{18}F-FMISO PET/CT becomes available, adaptive RT for tumor hypoxia might be used clinically.

Table 3. Characteristics of copper nuclides utilized in PET imaging and comparison with otherpositron emitters [59, 137-140]

Nuclides	$T_{1/2}$	Production	β^+ emission (E_{mean})	Other emissions	Range of β^+ in tissue	Use
Copper-60 (^{60}Cu)	23.7 min	Cyclotron	93% (0.970 MeV)	γ emission 1332 keV 88% 1791 keV 45.4%	4.4 mm	Diagnostic
Copper-61 (^{61}Cu)	3.33 h	Cyclotron	61% (0.500 MeV)	γ emission 282 keV 12.20% 656 keV 10.77%	2.6 mm	Diagnostic
Copper-62 (^{62}Cu)	9.67 min	Generator/cyclotron	97.83% (1.319 MeV)	γ emission 1172 0.74%	6.6 mm	Diagnostic
Copper-64 (^{64}Cu)	12.7 h	Cyclotron	17.6% (0.278 MeV)	γ emission 1345 keV 0.47% β- emission 0.190 MeV 38.7%	1.4 mm	Diagnostic/therapeutic
Fluoride-18 (^{18}F)	109.7 min	Cyclotron	96.7% (0.249 MeV)	β- emission (0.52 keV)	0.6 mm	Diagnostic
Iodine-124 (^{124}I)	4.17 days	Cyclotron	22.7% (0.820 MeV)	γ emission 0.602 keV 62.9% 1690.9 keV 11.15%	3 mm	Diagnostic
Gallium-68 (^{68}Ga)	67.71 min	Generator	88.91% (0.829 MeV)	γ emission 1077 keV 3.2%	2.9 mm	Diagnostic

Somewhat similar findings were reported in the study by Lee et al. [100], in which resolution of tumor hypoxia on mid-treatment ^{18}F-FMISO PET during fractionated RT, as would be expected for doses higher than 40 Gy, was consistent with the concept of reoxygenation. However, despite the promising results from the first report [45], neither the presence nor the absence of hypoxia defined by ^{18}F-FMISO PET during mid-treatment evaluation correlated with patient outcome.

More contradictory results have been reported in NSCLC. Lack of correlation between expression of tumor markers of hypoxia and ^{18}F-FMISO uptake was observed in a series of 17 patients with resectable NSCLC [37]. Gabel et al. [33] also found a lack of correlation between high initial tracer uptake and treatment response in NSCLC patients, although they reported that decreased ^{18}F-FMISO uptake at post-treatment evaluation was indicative of a favorable outcome. Evidence of utility of ^{18}F-FMISO PET in renal cell carcinoma or sarcoma is even more limited [36, 51, 101].

Taken together, these data raise a question mark over the use of ^{18}F-FMISO as a "universal" tracer for hypoxia imaging.

^{18}F-Fluoroazomycin arabinoside (^{18}F-FAZA)

The slow uptake of ^{18}F-FMISO in target tissue and slow clearance of unbound ^{18}F-FMISO from non-hypoxic areas stimulated the development of other tracers with improved pharmacokinetics, including ^{18}F-fluoroazomycin arabinoside (^{18}F-FAZA), a second-generation 2-nitroimidazole compound developed in 1999 [102]. Compared to ^{18}F-FMISO, the biodistribution of ^{18}F-FAZA is improved through the addition of a sugar moiety, making it less lipophilic [102, 103]. Souvatzoglou et al. [53] reported a higher contrast with non-target tissues for ^{18}F-FAZA compared to ^{18}F-FMISO, with an average tumor-to-muscle ratio of 2.0±0.3 at 2 h postinjection acquisition. The same group [104] had previously reported that ^{18}F-FAZA has overall superior pharmacokinetics and that use of dynamic analysis offers further potential improvement [105-107].

So far ^{18}F-FAZA has shown promising results in animal and patient studies [53, 102, 108-111] based on its selective accumulation in hypoxic tumors via a hypoxia-specific uptake mechanism [104]. In tumor-bearing mice with human SiHa cervix xenografts, for instance [112], intratumoral distribution of ^{18}F-FAZA was strongly correlated with the regional density of the pimonidazole-positive cells (pimonidazole being a hypoxia marker).

The role of tumor hypoxia depicted by ^{18}F-FAZA as a predictor of anticancer treatment response has been investigated in several preclinical models. The effect of hypoxia modulation with gefitinib, an epidermal growth factor receptor

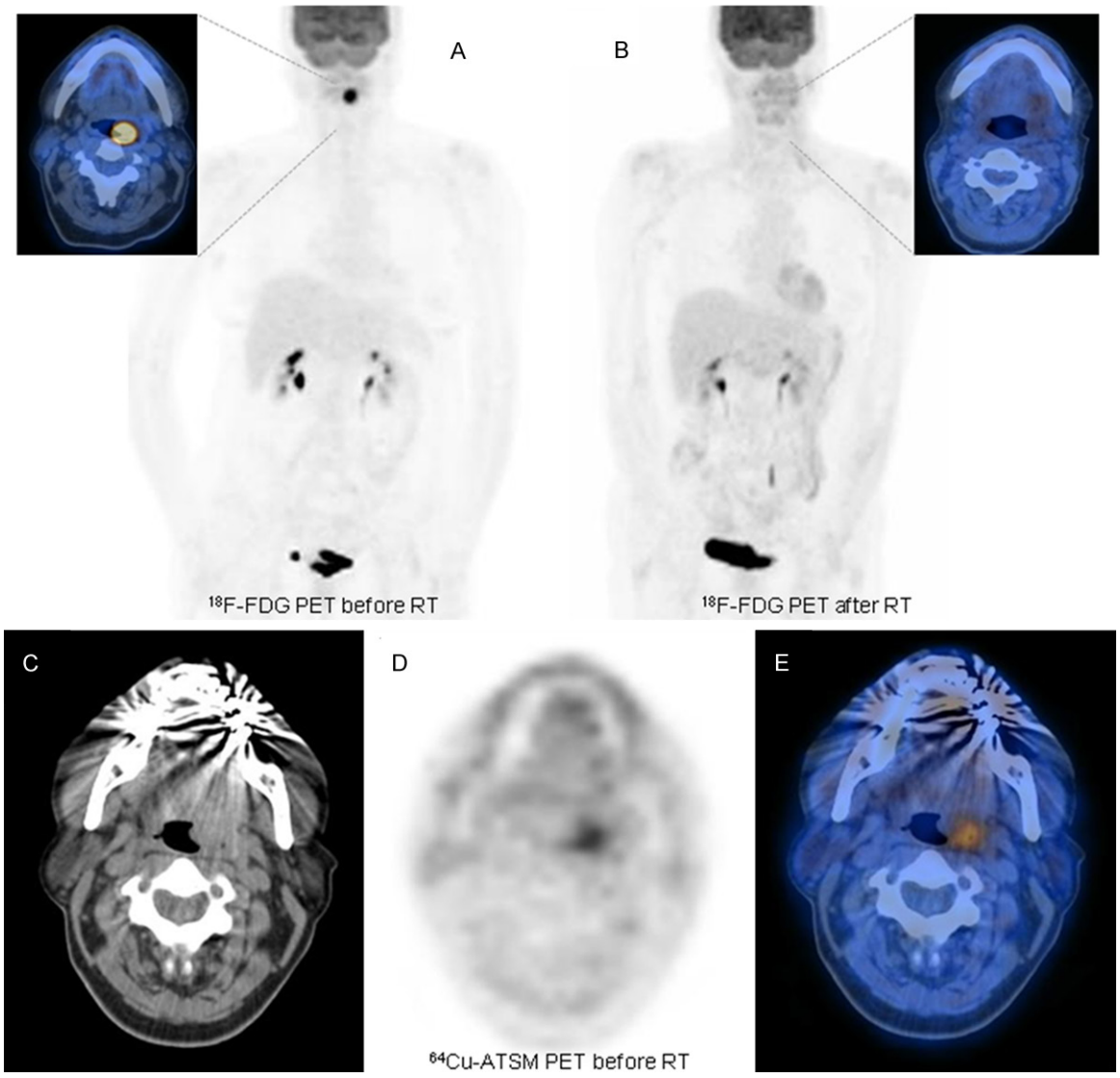

Figure 2. Example of a patient with localized head and neck squamous cell carcinoma (HNSCC) who was investigated with ^{18}F-FDG PET before (A) and after the end of RT (B). At staging the patient had undergone ^{64}Cu-ATSM PET/CT (C-E) documenting some mild uptake at the level of the primary tumor in the left tonsil (SUV_{max} 1.85). As is visible in (B) the patient achieved a complete response after treatment.

(EGFR) tyrosine kinase inhibitor, has been assessed with ^{18}F-FAZA PET in human EGFR-expressing A431 squamous cell carcinoma xenografts [113]. Also the use of radiosensitizers, such as tirapazamine, has been investigated with ^{18}F-FAZA PET in EMT6 tumor-bearing nude mice prior to treatment with concurrent chemoradiotherapy, RT alone, or chemotherapy alone [109]. In each case, hypoxia imaging proved efficient in predicting the beneficial effect of the treatment.

In a preclinical study, Mortensen et al. [114] investigated 92 female CDF1 mice with subcutaneous C3H mammary carcinomas prior to irradiation (55 Gy). The authors demonstrated a significant difference in local tumor control between "more hypoxic" and "less hypoxic" cases distinguished by either the median ^{18}F-FAZA tumor-to-blood ratio or the fraction of oxygen partial pressure at the pO_2 Eppendorf electrode.

These data, taken together, have prompted the investigation of ^{18}F-FAZA in clinical settings. One of the largest cohorts in which the tracer has been investigated in the clinical context is that reported by Postema et al. [115]. In a

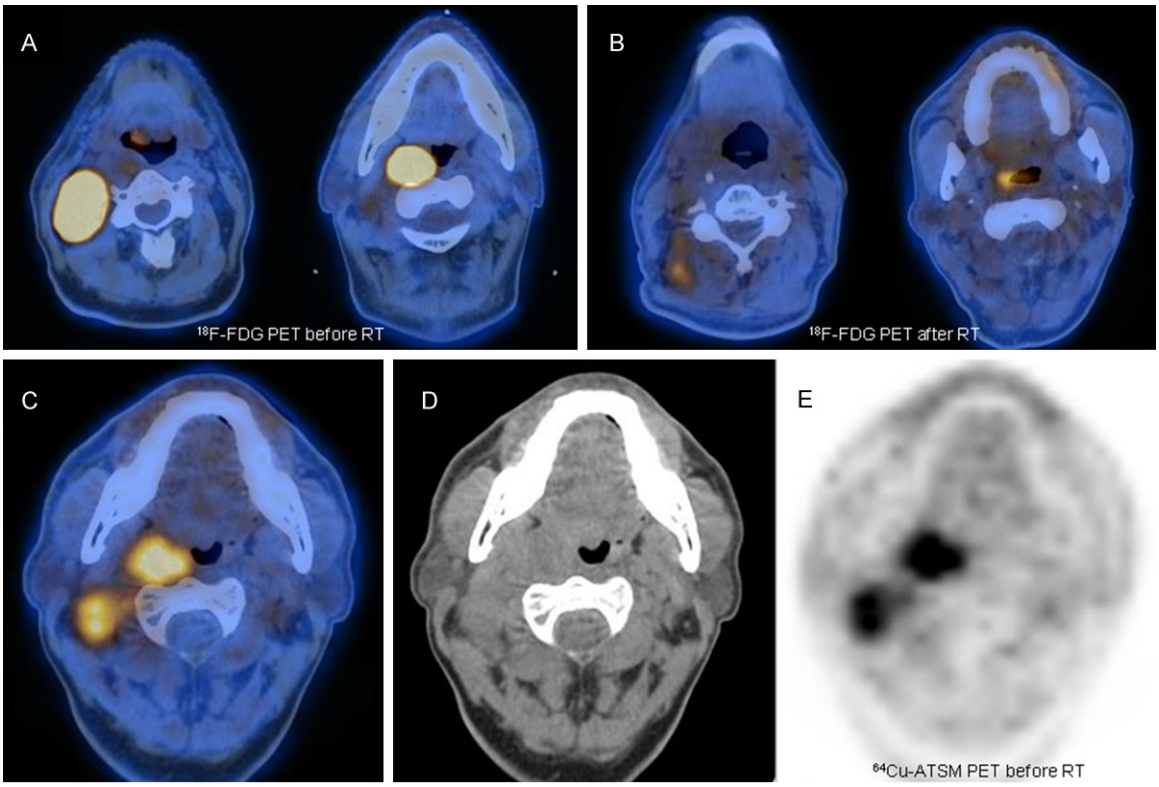

Figure 3. Example of a patient with advanced HNSCC who was investigated with ^{18}F-FDG PET at staging (A) and after the end of combined chemoradiotherapy (B). Before treatment the patient underwent ^{64}Cu-ATSM PET/CT (C-E), documenting intense tracer uptake (SUV_{max} 17.86) both in the primary tumor, involving the right tonsil, and in numerous bilateral cervical nodes. Despite the high-dose therapeutic regimen utilized, the patient presented some residual disease at end-of-treatment evaluation (B), as confirmed during follow-up.

group of 50 patients with different types of solid tumor, i.e., head and neck squamous cell carcinoma (HNSCC), small cell lung cancer (SCLC), NSCLC, malignant lymphoma, and high-grade gliomas, the authors aimed first to evaluate the safety and general biodistribution of ^{18}F-FAZA. They observed highly increased uptake of the tracer in all gliomas, with a tumor-to-background (T/B) ratio range of 1.9-15.6, and variable uptake in the remaining tumors, with a T/B closer to the average cut-off value of 1.6-2.0.

Recently, a group from Melbourne [56] investigated the role of ^{18}F-FAZA in 17 patients with locoregionally advanced NSCLC before concurrent chemoradiation. Intralesional hypoxia was identified in 65% of patients (11/17), and in those investigated with ^{18}F-FAZA PET after chemoradiation (60 Gy) (8/11), imageable hypoxia had resolved in the majority (6/8). Disease-free survival, however, did not differ significantly between patients with hypoxic and those with non-hypoxic tumors.

The first report on RT planning with ^{18}F-FAZA dates back to 2007 and focused on dose-painting according to hypoxia image-guided RT in 18 patients with advanced HNSCC [116]. In this report, Grosu et al. outlined the gross tumor volume (GTV) on ^{18}F-FAZA PET by applying a threshold of 50% with regard to background. This led to the inclusion of any PET-positive area with a T/M ratio ≥1.5. For primary localizations, GTV-FAZA presented with a single confluent hypoxic area in 61% of cases and with multiple diffused areas in 22%. In all cases, however, GTV-FAZA was inside the GTV outlined on CT. Although no comparison with ^{18}F-FDG distribution was performed to determine the effective benefit of GTV-PET delineation, the conclusion was that dose-painting on hypoxic areas is potentially feasible.

The use of ^{18}F-FAZA before RT also appears feasible in cervical cancer, as documented by Schuetz et al. [54], although the authors did not find a clear impact on survival in their limited cohort. Mortensen et al. [52] reported some

more thorough results from the DAHANCA 24 trial on the role of ^{18}F-FAZA PET in head and neck cancer before RT. The 40 patients investigated had undergone hypoxia PET before RT (66-76 Gy) and during treatment. In 25 cases (63%), PET showed a hypoxic volume with a tumor-to-muscle ratio (T/M) in the range of 1.1-2.9 (median 1.5). In this study, the prognostic significance of ^{18}F-FAZA PET was confirmed (p=0.04): at a median follow-up of 19 months, disease-free survival was 93% for patients with non-hypoxic tumors and 60% for patients with hypoxic tumors.

One of the open questions regarding hypoxia image-guided RT is the reproducibility of the PET data. Busk et al. [112] performed ^{18}F-FAZA PET twice before initiation of fractionated RT in mice bearing human SiHa cervix tumor xenografts and again following treatment. They found that ^{18}F-FAZA results were highly reproducible when based on injected dose, whereas normalization using an image-derived non-hypoxic reference tissue (i.e., muscle) yielded highly unreliable results. The authors underlined the stability of the intratumoral tracer distribution at baseline and its strong correlation with regional density of hypoxic cells. No evidence of general reoxygenation was observed during treatment, however, despite changes in overall tracer retention in individual mice. Consequently the question of reproducibility remains open when dealing with fractioned RT, especially with the intent of image-guided dose escalation.

Other nitroimidazole-like tracers

In view of the limitations of the above-mentioned compounds, other nitroimidazole-like tracers with high avidity for hypoxic tissue have been investigated and developed. One promising new radiopharmaceutical is ^{18}F-fluoroerythronitroimidazole (^{18}F-FETNIM), which is more hydrophilic than ^{18}F-FMISO and can be washed out more rapidly from well-oxygenated tissues, theoretically allowing a higher tumor-to-background ratio [117]. Pilot studies in patients with head and neck, esophageal, and lung cancer have demonstrated ^{18}F-FETNIM PET to be feasible and useful in hypoxia imaging [60, 61, 118], with the potential to predict response to treatment [118] and overall patient outcome [60]. Superior overall benefit in relation to ^{18}F-FMISO has not been demonstrated, however, and the T/B ratio for this tracer was not significantly superior to the ratios for other nitroimidazole-like tracers [119].

Similar results have been obtained with ^{18}F-fluoroetanidazole (^{18}F-FETA), which is a well-known nitroimidazole-like compound that has shown a better biodistribution than ^{18}F-FMISO owing to its lower levels of liver and lung retention [67, 68]. However, in spite of potential benefits, the diffusion of this tracer into tumor tissues appears limited [84].

Another group of hypoxia-avid radiopharmaceuticals, with a more stable but also more complex labeling chemistry, is represented by ^{18}F-2-nitroimidazol-pentafluoropropyl acetamide (^{18}F-EF5) and ^{18}F-2 nitroimidazol-trifluoropropyl acetamide (^{18}F-EF3) [66, 120, 121]. These tracers are slightly more lipophilic than the formerly described compounds and have been investigated in animal models as well as in clinical studies on head and neck cancer and cervical and brain tumors [62-64]. For these tracers, too, the optimal tumor-to-muscle cut-off value is low (T/M 1.5) and the potential advantage over ^{18}F-FMISO is still negligible.

Valuable alternatives may be biochemically similar tracers labeled with other nuclides, including iodine-124 (^{124}I), e.g., ^{124}I-iodoazomycin galactopyranoside (^{124}I-IAZG) [69], and gallium-68 (^{68}Ga), e.g., ^{68}Ga-NOTA-nitroimidazole, ^{68}Ga-DOTA-nitroimidazole, and ^{68}Ga-SCN-NOTA-nitroimidazole [70, 71] (**Table 2**). The ^{68}Ga-labeled tracers have the additional advantage of utilizing a nuclide produced by a generator (^{68}Ga/^{68}Ge) and are thus potentially applicable in PET centers without an onsite cyclotron. Up to now, however, these tracers have not proved superior to the principal nitroimidazole representative, ^{18}F-FMISO, for hypoxia imaging. As a consequence, their application is still limited to preclinical studies [70, 71, 84].

Non-nitroimidazole compounds

Cu-diacetyl-bis(N4-methylthiosemicarbazone) (Cu-ATSM)

Radioactive copper (^{60,61,62,64}Cu) labeled with diacetyl-bis(*N*4-methylthiosemicarbazone) (Cu-ATSM) is a very promising PET radiopharmaceutical for hypoxia imaging. First investigated for

this purpose in 1997 [122], the compound appeared immediately suitable for detection of hypoxia in living tissue. A series of copper radioisotopes is now available for labeling ATSM, each with its specific half-life ($T_{1/2}$), decay scheme, and production facilities (**Table 3**). The mechanism of uptake is still not fully understood, but as Fujibayashi et al. suggested [122], retention of the tracer in tumor cells is principally dependent on cytosolic/microsomal bioreduction [123]. In fact Cu-ATSM is a neutral lipophilic molecule, which is highly membrane permeable and can passively diffuse within the intracellular environment (**Figure 1**). Once inside the cell, the bivalent copper compound, Cu(II)-ATSM, undergoes reduction by thiols and is converted into Cu(I)-ATSM complex [124]. In hypoxic conditions this complex, less stable than the bivalent form, is progressively dissociated into H_2-ATSM and free Cu(I), which is rapidly entrapped in intracellular proteins [122, 125]. The entrapment is reported to reflect the level of tissue oxygenation in many tumor types [34, 72-74, 76, 78] and when directly compared to the principal 2-nitroimidazole family representative (^{18}F-FMISO), Cu-ATSM uptake is significantly higher in target tissue than in non-hypoxic areas and occurs at an earlier time (10-15 min versus 2-4 h) [88, 126]. These data have also been confirmed in relation to other nitroimidazole compounds, i.e., ^{18}F-FAZA and ^{18}F-HX4 [99], in nude mice bearing human xenografts.

From recent investigations, it appears plausible that a significant role in the Cu-ATSM entrapment is played by copper itself. To test this assumption, Hueting et al. [127] analyzed the in vitro and in vivo distribution of ^{64}Cu-ATSM and ^{64}Cu-acetate in the same animal models (EMT6 and CaNT). They showed a similar tissue distribution of radio-copper for both tracers and suggested that copper metabolism can play a role in the mechanism of selectivity of Cu-ATSM in hypoxia. More thorough investigations and consolidated evidence in the clinical context are required to confirm these data.

The first human use of Cu-ATSM dates back to 2000, when Takahashi et al. [128] studied its application in four normal subjects and six patients with lung cancer. The tracer, in this case ^{62}Cu-ATSM, accumulated within a few minutes in all patients with cancer, giving a tumor-to-background ratio of 3.0, whereas it rapidly cleared from the blood of all normal subjects. Similar findings have been documented for the other copper radioisotopes labeled with ATSM. In their feasibility study, Dehdashti et al. [34] analyzed the role of ^{60}Cu-ATSM in patients with NSCLC and correlated imaging findings with follow-up (n=19) and response to therapy (n=14). As expected, the tracer had a variable distribution in tumor masses, depending on hypoxia level, and the authors were able to define a tumor-to-muscle (T/M) ratio of 3.0 as effective in distinguishing treatment responders from non-responders.

The same group [74] evaluated the prognostic significance of ^{60}Cu-ATSM in 14 patients with cervical cancer before RT and chemotherapy. This time the selected T/M ratio was 3.5, which could optimally distinguish patients experiencing recurrence from those free of disease at last follow-up. Similar results were obtained in a more recent study in 38 patients with cervical carcinoma [128]. In this case, ^{60}Cu-ATSM performed before treatment gave relevant information on tumor oxygenation and was predictive of patient outcome.

The group from Yokohama City University [72] investigated use of ^{62}Cu-ATSM in 17 patients with locally advanced head and neck cancer (stage III and IV) prior to chemotherapy or RT. In 15 cases the authors assessed the relationship between clinical outcome and ^{62}Cu-ATSM uptake. The SUV_{max} in their analysis differed significantly ($p < 0.05$) in patients free of disease at 2 years postirradiation follow-up versus those with residual/recurrent disease. More specifically, all cured patients had a SUV_{max} <5.0 and all patients (n=10) with persistent disease had a SUV_{max} >5.0 (**Figures 2** & **3**).

Recently ^{62}Cu-ATSM was investigated in 22 patients with gliomas [78] with the intent of differentiating tumor grade according to uptake and correlating findings with contrast-enhanced regions on MRI and HIF-1α expression at immunohistochemistry. Using a tumor-to-background ratio threshold of 1.8 at 30-40 min post injection, ^{62}Cu-ATSM uptake was found to be predictive of HIF-1α expression, with 92.3% sensitivity and 88.9% specificity. Moreover, it correlated significantly with the presence of a necrotic component (p=0.002) and defined regional uptake in 61.9% (13/21) of tumors within the contrast-enhanced region on MRI.

However, other preclinical data suggest that Cu-ATSM may not be suitable for hypoxia detection in all types of tumor. In a fibrosarcoma animal model (FSA) and in prostate cancer cell lines (PC-3, 22Rv1, LNCaP, LAPC-4, and R3327-AT) [130-132], the tracer showed limited selectivity for hypoxia, suggesting the need for specific tumor-type studies with Cu-ATSM and also for more clinical evidence in these types of solid tumor. This latter aspect is crucial because animal models do not completely match human cancer and tend to give discordant findings based on the cell line utilized. For example, the rat model of fibrosarcoma investigated by Jalilian et al. in 2009 [133] with ^{61}Cu-ATSM yielded completely different results from the findings of Yuan et al [130] using the FSA model.

With regard to RT planning, the principal advantage of Cu-ATSM is its high tumor-to-background ratio (T/B >3.0). As reported by Dalah et al. [134] in their simulation of tissue activity curves for ^{64}Cu-ATSM and ^{18}F-FMISO for sub-target volume delineation, a good tumor-to-background ratio allows high sensitivity and specificity targeting of positive lesions on PET. This was also shown in the feasibility study reported by Chao et al [135] in head and neck tumors, where the use of IMRT based on Cu-ATSM led to a higher dose (80 Gy) in hypoxic areas and spared more than half of the parotid glands to less than 30 Gy [116]. However, one weakness of ^{64}Cu-ATSM needs to be underlined: the total body irradiation at diagnostic administered activities (500-800 MBq) is twice as high as the dose calculated for ^{18}F-FMISO [59, 136].

Nevertheless, among the different copper nuclides, ^{64}Cu represents the best compromise based on $T_{1/2}$, intrinsic image resolution and production yield (**Table 3**). In a direct comparison of ^{60}Cu-ATSM and ^{64}Cu-ATSM in ten patients with cervical carcinoma [75], for instance, ^{64}Cu-ATSM proved as safe as ^{60}Cu-ATSM while also offering the advantage of better image quality. Another advantage of the use of ^{64}Cu-ATSM is the theranostic potential of the nuclide, which emits medium-energy β- particles, along with positrons, and produces high linear energy transfer (LET) Auger electrons [136, 141]. At adequate doses and thanks to the short path length of the emissions, the nuclide can produce a toxic effect on targeted cells with minimal effects on neighboring tissue, as already reported in some preclinical studies [141, 142]. This therapeutic effect could also be seen by Yoshii et al. [143] in a mouse colon carcinoma (Colon-26) model, where ^{64}Cu-ATSM administration at 37 MBq twice a week reduced tumor volume as well as the percentage of CD133+ cells and the metastatic ability of Colon-26 tumors. However, this potential application needs more clinical evidence, so that for the time being the major use of ^{64}Cu-ATSM in the diagnostic field is for hypoxia assessment.

^{124}I-cG250 and ^{89}Zr-cG250-F(ab′)

Carbonic anhydrase IX (or CAIX) is a transmembrane enzyme involved in the cellular regulation of pH homeostasis and represents one of the downstream targets of HIF-1α [81]. Its role is to hydrolyze the carbon dioxide (CO_2) into carbonic acid (H_2CO_3) and stabilize intracellular pH [81, 144]. With the exception of renal cell carcinoma, where the CAIX expression is not related to hypoxia, in tumors this enzyme is up-regulated as a result of reduced levels of oxygenation, namely <20 mmHg, and can therefore be targeted for hypoxia imaging [79, 81, 145].

The first compound developed for the identification of CAIX, although at the time the enzyme was not known, was the antibody Grawitz250 (G250) [146]. Later the chimeric version of the antibody was labeled with ^{124}I-iodine as a tracer for PET imaging (^{124}I-cG250) [79, 147], and more recently selected antibody fragments have been labeled with ^{89}Zr-zirconium (^{89}Zr-cG250-F(ab′) for the same purpose [81]. This category of tracers has the potential to detect hypoxia in tumors, other than renal cell carcinoma, owing to the good correlation reported between tracer uptake and CAIX expression, although the evidence is still too limited and is reliant only on preclinical studies.

Conclusions

The clinical relevance of hypoxia in patients with cancer means that it has the potential to become a useful prognostic biomarker. Furthermore, the possibility of identifying hypoxia in vivo without any invasive intervention may be of great value in improving treatment. Among the numerous PET tracers investigated, a broad range of radiopharmaceuticals

have been found to specifically identify hypoxia expression in tumors. It is nevertheless not straightforward to determine the most useful tracer for this purpose because many factors influence the choice. Evidence-based data favor the use of ^{18}F-FMISO, but the issue of suboptimal imaging persists. On the other hand, if importance is placed on high PET image quality, ^{64}Cu-ATSM would be selected; in this case, however, evidence is more limited and the mechanism of uptake in hypoxic tissue is still not completely clear. Alternatively, "new" tracers labeled with cyclotron-independent nuclides hold appeal despite the apparent lack of superiority compared to ^{18}F-FMISO. Nonetheless, if a "winner" has to be chosen in this "competition", we would select the tracer that demonstrates better image quality.

Disclosure of conflict of interest

None to declare.

Address correspondence to: Egesta Lopci, Department of Nuclear Medicine, University Hospital S. Orsola-Malpighi, Via Massarenti, 9 - 40138 Bologna, Italy; Department of Nuclear Medicine, Humanitas Clinical and Research Center, Via Manzoni, 56 - 20089 Rozzano (MI), Italy. Tel: +39 02 82247542; Fax: +39 02 82246693; E-mail: egesta.lopci@cancercenter.humanitas.it; egesta.lopci@gmail.com

References

[1] Vaupel P, Mayer A. Hypoxia in cancer: significance and impact on clinical outcome. Cancer Metastasis Rev 2007; 26: 225-239.

[2] Tomlinson RH, Gray LH. The histological structure of some human lung cancers and the possible implications for radiotherapy. Br J Cancer 1955; 9: 539-49.

[3] Mees G, Dierckx R, Vangestel C, Van de Wiele C. Molecular imaging of hypoxia with radiolabelled agents. Eur J Nucl Med Mol Imaging 2009; 36: 1674-1686.

[4] Anderson CJ, Ferdani R. Copper-64 radiopharmaceuticals for PET imaging of cancer: advances in preclinical and clinical research. Cancer Biother Radiopharm 2009; 24: 379-393.

[5] Albiach CF, Moreno AC, Cordon MR, Morillo Macías V, Bouché Babiloni A, Beato Tortajada I, Sánchez Iglesias A, Francés Muñoz A. Contribution of hypoxia-measuring molecular imaging techniques to radiotherapy planning and treatment. Clin Transl Oncol 2010; 12: 22-26.

[6] Rajendran JG, Hendrickson K, Spence A, Muzi M, Krohn KA, Mankoff DA. Hypoxia imaging directed radiation treatment planning. Eur J Nucl Med Mol Imaging 2006; 33 Suppl 1: 44-53.

[7] Vaupel P, Harrison L. Tumor hypoxia: causative factors, compensatory mechanisms, and cellular response. Oncologist 2004; 9 Suppl 5: 4-9.

[8] Post DE, Van Meir EG. Generation of bidirectional hypoxia7HIF-responsive expression vectors to target gene expression to hypoxic cells. Gene Ther 2001; 8: 1801-1807.

[9] Krause BJ, Beck R, Souvatzoglou M, Piert M. PET and PET/CT studies of tumor tissue oxygenation. Q J Nucl Med Mol Imaging 2006; 50: 28-43.

[10] Hoeckel M, Knoop C, Schlenger K, Vorndran B, Baussmann E, Mitze M, Knapstein PG, Vaupel P. Intratumoral pO2 predicts survival in advanced cancer of the uterine cervix. Radiother Oncol Jan 1993; 26: 45-50.

[11] Padhani AR. Where are we with imaging oxygenation in human tumors? Cancer Imaging 2005; 5: 128-130.

[12] Hockel M, Vaupel P. Tumor hypoxia: definitions and current clinical, biologic, and molecular aspects. J Natl Cancer Inst 2001; 93: 266-76.

[13] Evans SM, Koch CJ. Prognostic significance of tumor oxygenation in humans. Cancer Lett 2003; 195: 1-16.

[14] Vikram DS, Zweier JL, Kuppusamy P. Methods for noninvasive imaging of tissue hypoxia. Antioxidant Redox Signal 2007; 9: 1745-1756.

[15] Lapi SE, Voller TF, Welch MJ. Positron Emission Tomogtaphy Imaging of Hypoxia. PET Clin 2009; 1: 39-47.

[16] Krohn KA, Link JM, Mason RP. Molecular Imaging of Hypoxia. J Nucl Med 2008; 49: 129S-148S.

[17] Egeland TAM, Gulliksrud K, Gaustad JV, Mathiesen B, Rofstad EK. Dynamic constrast-enhanced-MRI of tumor hypoxia. Magn Reson Med 2012; 67: 519-530.

[18] Manzoor AA, Yuan H, Palmer GM, Viglianti BL, Dewhirst MW. Imaging Hypoxia. Molecular Imaging: Principles and Practice. Edited by Weissleder R, Ross BD, Rehemtulla A, Gambhir SS. Shelton: PMPH-USA 2010; pp: 756-779.

[19] Wang W, Lee NY, Georgi J, Narayanan M, Guillem J, Schöder H, Humm JL. Pharmacokinetic analysis of hypoxia 18F-fluoromisonidazole dynamic PET in head and neck cancer. J Nucl Med 2010; 51: 37-45.

[20] Price JM, Robinson SP, Koh DM. Imaging hypoxia in tumours with advanced MRI. Q J Nucl Med Mol Imaging 2013; 57: 257-70.

[21] Chapman JD, Franko AJ, Sharplin J. A Marker for Hypoxic Cells in Tumors with Potential Clini-

cal Applicability. British Journal of Cancer 1981; 43: 546-50.
[22] Dierckx RA, Van de Wiele. FDG uptake, a surrogate of tumour hypoxia? Eur J Nucl Med Mol Imaging 2008; 35: 1544-9.
[23] Van Baardwijk A, Dooms C, van Suylen RJ, Verbeken E, Hochstenbag M, Dehing-Oberije C, Rupa D, Pastorekova S, Stroobants S, Buell U, Lambin P, Vansteenkiste J, de Ruysscher D. The maximum uptake of (18)F-deoxyglucose on positron emission tomography scan correlated with survival, hypoxia inducible factor-1alpha and GLUT-1 in non-small cell lung cancer. Eur J Cancer 2007; 43: 1392-8.
[24] Clavo AC, Brown RS, Wahl RL. Fluorodeoxyglucose uptake in human cancer cell lines is increase by hypoxia. J Nucl Med 1995; 36: 1625-32.
[25] Busk M, Horsman MR, Kristjansen PEG, van der Kogel AJ, van der Kogel AJ, Bussink J, Overgaard J. Aerobic glycolisis in cancer: implications for the usability of oxygen-responsive genes and fluorodeoxyglucose-PET as markers of tissue hypoxia. Int J Cancer 2008; 122: 2726-2734.
[26] Warburg O. On respiratory impairment in cancer cells. Science 1956; 124: 269-70.
[27] Kaira K, Okumura T, Ohde Y, Takahashi T, Murakami H, Oriuchi N, Endo M, Kondo H, Nakajima T, Yamamoto N. Correlation between 18F-FDG uptake on PET and molecular biolgy in metastatic pulmonary tumors. J Nucl Med 2011; 52: 705-11.
[28] Airley RE, Mobasheri A. Hypoxic regulation of glucose transport, anaerobic metabolism and angiogenesis in cancer: noverl pathways and targets for anticancer therapeutics. Chemotherapy 2007; 53: 233-56.
[29] Kim JW, Gao P, Dang CV. Effects of hypoxia on tumor metabolism. Cancer Metastasis Rev 2007; 26: 291-8.
[30] Christian N, Deheneffe S, Bol A, DeBast M, Labar D, Lee JA, Gregoire V. Is 18F-FDG a surrogate tracer to measure tumor hypoxia? Comparison with the hypoxic tracer 14C-EF3 in animal tumor models. Radiother Oncol 2010; 97: 183-8.
[31] Zimny M, Gagel B, DiMartino E, Hamacher K, Coenen H, Westhofen M, Eble M, Buell U, Reinartz P. FDG-a marker of tumour hypoxia? A comparison with [(18)F]fluoromisonidazole and pO2-polarography in metastatic head and neck cancer. Eur J Nucl Med Mol Imaging 2006; 33: 1426-31.
[32] Gabel B, Reinartz P, DiMartino E, Zimny M, Pinkawa M, Maneschi P, Stanzel S, Hamacher K, Coenen HH, Westhofen M, Bull U, Eble MJ. pO2 Polarography Versus Positron Emission Tomography ([18F]Fluoromisonidazole, [18F]-2-Fluoro-2'-Deoxyglucose). Strahlenther Onkol 2004; 180: 616-22.
[33] Gabel B, Reinartz P, Demirel C, Kaiser HJ, Zimny M, Piroth M, Pinkawa M, Stanzel S, Asadpour B, Hamacher K, Coenen HH, Buell U, Eble MJ. [18F]fluoromisonidazole and [18F]fluorodeoxyglucose positron emission tomography in response evaluation after chem.-/radiotherapy of non-small-cell lung cancer: a feasibility study. BMC Cancer 2006; 6: 51.
[34] Dehdashti F, Mintun MA, Lewis JS, Bradley J, Govidan R, Laforest R, Welch MJ, Siegel BA. In vivo assessment of tumor hypoxia in lung cancer with 60Cu-ATSM. Eur J Nucl Med Mol Imaging 2003; 30: 844-50.
[35] Thorwarth D, Eschmann SM, Holzner F, Paulsen F, Alber M. Combined uptake of [18F] FDG and [18F]FMISO correlates with radiation therapy outcome in head-and-neck cancer patients. Radiother Oncol 2006; 80: 151-56.
[36] Rajendran JG, Wilson DC, Conrad EU, Peterson LM, Bruckner JD, Rasey JS, Chin LK, Hofstrand PD, Grierson JR, Eary JF, Krohn KA. [18F]FMISO and [18F]FDG PET imaging in soft tissue sarcomas correlation of hypoxia, metabolism and VEGF expression. Eur J Nucl Med Mol Imaging 2003; 30: 695-704.
[37] Cherk MH, Foo SS, Poon AMT, Knight SR, Murone C, Papenfuss AT, Sachinidis JI, Saunder THC, O'Keefe GJ, Scott AM. Lack of correlation of hypoxic cell fraction and angiogenesis with glucose metabolic rate in non-small cell lung cancer assessed by 18F-Fluoromisonidazole and 18F-FDG PET. J Nucl Med 2006; 47: 1921-1926.
[38] Cher L, Murone C, Lawrentschuk N, Ramdave S, Papenfusse A, Hannah A, O'keefe GJ, Sachinidis JL, Berlangieri SU, Fabinyi G, Scott AM. Correlation of hypoxic cell fraction and angiogenesis with glucose metabolic rate in gliomas using 18F-fluoromisonidazole, 18F-FDG PET, and immunohistochemical studies. J Nucl Med 2006; 47: 410-18.
[39] Takebayashi R, Izuichi K, Yamamoto Y, Kameyama R, Mori H, Masaki T, Suzuki Y. [18F] fluorodeoxyglucose accumulation as a biological marker of hypoxic status but not glucose transport ability in gastric cancer. J Exp Clin Can Res 2013; 32: 34.
[40] Han MW, Lee HJ, Cho KJ, Kim JS, Roh JL, Choi SH, Nam SY, Kim SY. Role of FDG-pet as a biological marker for predictiong the hypoxic status of tongue cancer. Head Neck 2012; 34: 1395-1402.
[41] Yamada T, Uchida M, Kwang-Lee K, Kitamura N, Yoshimura T, Sasabe E, Yamamoto T, Japan K. Correlation of metabolism7hypoxia markers and fluorodeoxyglucose uptake in oral squamous cell carcinomas. Oral Surg Oral Med Oral Pathol Oral Radiol 2012; 113: 464-71.

[42] Eschmann SM, Paulsen F, Reimold M, Dittmann H, Welz S, Reischl G, Machulla HJ, Bares R. Prognostic impact of hypoxia imaging with 18F-misonidazole PET in non-small cell lung cancer and head and neck cancer before radiotherapy. J Nucl Med 2005; 46: 253-60.

[43] Rajendran JG, Schwartz DL, O'Sullivan J, Peterson LM, Ng P, Scharnhorst J, Grierson JR, Krohn KA. Tumor hypoxia imaging with [F-18] Fluoromisonidazole positron emission tomography in head and neck cancer. Clin Cancer Res 2006; 12: 5435-41.

[44] Kikuchi M, Yamane T, Shinohara Sh, Fujiwara K, Hori SY, Tona Y, Yamazaki H, Naito Y, Senda M. 18F-fluoromisonidazole positron emission tomography before treatment is a predictor of radiotherapy outcome and survival prognosis in patients with head and neck squamous cell carcinoma. Ann Nucl Med 2011; 25: 625-633.

[45] Lee NY, Mechalakos JG, Nehmeh S, Lin Z, Squire OD, Cai S, Chan K, Zanzonico PB, Greco C, Ling CC, Humm JL, Schöder H. Fluorine-18-labeled fluoromisonidazole positron emission and computed tomography-guided intensity-modulated radiotherapy for head and neck cancer: a feasibility study. Int J Radiat Oncol Biol Phys 2008; 70: 2-13.

[46] Zips D, Zoephel K, Abolmaali N, Perrin R, Abramyuk A, Haase R, Appold S, Steinbach J, Kotzerke J, Baumann M. Exploratory prospective trial of hypoxia-specific PET imaging during radiochemotherapy in patients with locally advanced head-and-neck cancer. Radiother Oncol 2012; 105: 21-28.

[47] Spence AM, Muzi M, Swanson KR, O'Sullivan F, Rockhill JK, Rajendran JG, Adamsen TC, Link JM, Swanson PE, Yagle KJ, Rostomily RC, Silbergeld DL, Krohn KA. Regional hypoxia in glioblastoma multiforme quantified with [18F]fluoromisonidazole positron emission tomography before radiotherapy: correlation with time to progression and survival. Clin Cancer Res 2008 May 1; 14: 2623-30.

[48] Hirata K, Terasaka SH, Shiga T, Hattori N, Magota K, Kobayashi H, Yamaguchi S, Houkin K, Tanaka S, Kuge Y, Tamaki N. 18F-Fluoromisonidazole positron emission tomography may differentiate glioblastoma multiforme from less malignant gliomas. Eur J Nucl Med Mol Imaging 2012; 39: 760-770.

[49] Cheng J, Lei L, Xu J, Sun Y, Zhang Y, Wang X, Pan L, Shao ZH, Zhang Y, Liu G. 18F-Fluoromisonidazole PET/CT: a potential tool for predicting primary endocrine therapy resistance in breast cancer. J Nucl Med 2013; 54: 333-40.

[50] Rasey JS, Koh WJ, Evans ML, Peterson LM, Lewellen TK, Graham MM, Krohn KA. Quantifying regional hypoxia in human tumors with positron emission tomography of [18F]fluoromisonidazole: a pretherapy study of 37 patients. Int J Radiat Oncol Biol Phys 1996; 36: 417-428.

[51] Lawrentschuk N, Poon AMT, Foo SS, Jonhs LG, Putra J, Murone C, Davis ID, Bolton DM, Scott AM. Assessing regional hypoxia in human renal tumours using 18F-fluoromisonidazole positron emission tomography. BJU International 2005; 96: 540-546.

[52] Mortensen LS, Johansen J, Kallehauge J, Primdahl H, Busk M, Lassen P, Alsner J, Sorensen BS, Toustrup K, Jakobsen S, Petersen J, Petersen H, Theil J, Nordsmark M, Overgaard J. FAZA PET/CT hypoxia imaging in patients with squamous cell carcinoma of the head and neck treated with radiotherapy: results from the DAHANCA 24 trial. Radiother Oncol 2012; 105: 14-20.

[53] Souvatzoglou M, Grosu AL, Roeper B, Krause BJ, Beck R, Reischl G, Picchio M, Machulla HJ, Wester HJ, Piert M. Tumour hypoxia imaging with [18F]FAZA PET in head and neck cancer patients: a pilot study. Eur J Nucl Med Mol Imaging 2007; 34: 1566-75.

[54] Schuetz M, Schmid MP, Potter R, Kommata S, Georg D, Lukic D, Dudczak R, Kletter K, Dimopoulos J, Karanikas G, Bachtiary B. Evaluating repetitive 18F-fluoroazomycin-arabinozide (18F-FAZA) PET in setting of MRI guided adaptive radiotherapy in cervical cancer. Acta Oncol 2010; 49: 941-947.

[55] Garcia-Parra R, Wood D, Shah RB, Siddiqui J, Hussain H, Park H, Desmond T, Meyer C, Piert M. Investigation on tumor hypoxia in resectable primary prostate cancer as demonstrated by 18F-FAZA PET/CT utilizing multimodality fusion techniques. Eur J Nucl Med Mol Imaging 2011; 38: 1816-1823.

[56] Trinkaus ME, Blum R, Rischin D, Callahan J, Bressel M, Segard T, Roselt P, Eu P, Binns D, MacManus MP, Ball D, Hicks RJ. Imaging of hypoxia with 18F-FAZA PET in patients with locally advanced non-small cell lung cancer treated with definitive chemoradiotherapy. J Med Imaging Radiat Oncol 2013 Aug; 57: 475-81.

[57] Bollineni VR, Kerner GS, Pruim J, Steenbakkers RJ, Wiegman EM, Koole MJ, de Groot EH, Willemsen AT, Luurtsema G, Widder J, Groen HJ, Langendijk JA. PET imaging of tumor hypoxia using 18F-fluoroazomycin arabinoside in stage III-IV non-small cell lung cancer patients. J Nucl Med 2013 Aug; 54: 1175-80.

[58] Havelund BM, Holdgaard PC, Rafaelsen SR, Mortensen LS, Theil J, Bender D, Pløen J, Spindler KL, Jakobsen A. Tumour hypoxia imaging with 18F-fluoroazomycinarabinofuranoside PET/CT in patients with locally advanced rectal cancer. Nucl Med Commun 2013 Feb; 34: 155-61.

[59] Bourgeois M, Rajerison H, Guerard F, Mougin-Degraef M, Barbet J, Michel N, Cherel M, Faivre-Chauvet A. Contribution of [64Cu]-ATSM PET in molecular imaging of tumour hypoxia compared to classical [18F]-MISO–a selected review. Nucl Med Rev Cent East Eur 2011; 14: 90-5.

[60] Li L, Hu M, Zhu H, Zhao W, Yang G, Yu J. Comparison of 18F-Fluoroerythronitroimidazole and 18F-Fluorodeoxygucose Positron Emission Tomography and Prognostic Value in Locally Advanced Non-Small-Cell Lung Cancer. Clin Lung Canc 2010; 11: 335-340.

[61] Yue J, Yang Y, Cabrera AR, Sun X, Zhao S, Xie P, Zheng J, Ma L, Fu Z, Yu J. Measuring tumor hypoxia in esophageal squamous cell carcinoma: a pilot clinical study. Dis Esophagus 2012; 25: 54-61.

[62] Evans SM, Judy KD, Dunphy I, Jenkins WT, Nelson PT, Collins R, Wileyto EP, Jenkins K, Hahn SM, Stevens CW, Judkins AR, Phillips P, Geoerger B, Koch CJ. Comparative measurements of hypoxia in human brain tumors using needle electrodes and EF5 binding. Cancer Res 2004 64: 1886-1892.

[63] Evans SM, Fraker D, Hahn SM, Gleason K, Jenkins WT, Jenkins K, Hwang WT, Zhang P, Mick R, Koch CJ. EF5 binding and clinical outcome in human soft tissue sarcomas. Int J Radiat Oncol Biol Phys 2006; 64: 922-927.

[64] Komar G, Seppanen M, Eskola O, Lindholm P, Grönroos TJ, Forsback S, Sipilä H, Evans SM, Solin O, Minn H. F-18-EF5: A New PET Tracer for Imaging Hypoxia in Head and Neck Cancer. J Nucl Med 2008; 49: 1944-1951.

[65] Dubois L, landuyt W, Cloetens L, Bol A, Bormans G, Haustermans K, Labar D, Nuyts J, Grégoire V, Mortelmans L. [18F]EF3 is not superior to [18F]FMISO for PET-based hypoxia evaluation as measured is a rat rhabdomyosarcoma tumour model. Eur J Nucl Med Mol Imaging 2009; 36: 209-218.

[66] Mahy P, De Bast M, de Groot T, Cheguillaume A, Gillart J, Haustermans K, Labar D, Grégoire V. Comparative pharmacokinetics, biodistribution, metabolism and hypoxia-dependent uptake of [18F]-EF3 and [18F]-MISO in rodent tumor models. Radiother Oncol 2008 Dec; 89: 353-60.

[67] Rasey JS, Hofstrand PD, Chin LK, Tewson TJ. Characterization of [F-18]fluoroetanidazole, a new radiopharmaceutical for detecting tumor hypoxia. J Nucl Med 1999; 40: 1072-1079.

[68] Barthel H, Wilson H, Collingridge DR, Brown G, Osman S, Luthra SK, Brady F, Workman P, Price PM, Aboagye EO. In vivo evaluation of [18F]fluoroetanidazole as a new marker for imaging tumour hypoxia with positron emission tomography. Br J Cancer 2004; 90: 2232-2242.

[69] Riedl CC, Brader P, Zanzonico P, Reid V, Woo Y, Wen B, Ling CC, Hricak H, Fong Y, Humm JL. Tumor hypoxia imaging in orthotopic liver tumors and peritoneal metastasis: a comparative study featuring dynamic 18F-MISO and 124I-IAZG PET in the same study cohort. Eur J Nucl Med Mol Imaging 2008; 35: 39-46.

[70] Hoigebazar L, Jeong JM, Choi SY, Choi JY, Shetty D, Lee YS, Lee DS, Chung JK, Lee MC, Chung YK. Synthesis and characterization of nitroimidazole derivatives for Ga-68-labeling and testing in tumor xenografted mice. J Med Chem 2010; 53: 6378–6385.

[71] Hoigebazar L, Jeong JM, Hong MK, Kim YJ, Lee JY, Shetty D, Lee YS, Lee DS, Chung JK, Lee MC. Synthesis of (68)Ga-labeled DOTA-nitroimidazole derivatives and their feasibilities as hypoxia imaging PET tracers. Bioorg Med Chem 2011; 19: 2176-2181.

[72] Minagawa Y, Shizukuishi K, Koike I, Horiuchi C, Watanuki K, Hata M, Omura M, Odagiri K, Tohnai I, Inoue T, Tateishi U. Assessment of tumor hypoxia by 62Cu-ATSM PET/CT as a predictor of response in head and neck cancer: a pilot study. Ann Nucl Med 2011; 25: 339-345.

[73] Grassi I, Nanni C, Cicoria G, Blasi C, Bunkheila F, Lopci E, Colletti PM, Bubello D, Fanti S. Usefulness of 64CU-ATSM in Head and Neck Cancer: A preliminary Prospective Study. Clin Nucl Med 2014; 39: e59-63.

[74] Dehdashti F, Grigsby PW, Mintun MA, Lewis JS, Siegel BA, Welch MJ. Assessing tumor hypoxia in cervical cancer by positron emission tomography with 60Cu-ATSM: relationship to therapeutic response - a preliminary report. Int J Radiation Oncology Biol Phys 2003; 55: 1233-38.

[75] Lewis JS, Laforest R, Dehdashti F, Grigsby PW, Welch MJ, Siegel BA. An Imaging comparison of 64Cu-ATSM ad 60Cu-ATSM in cancer of uterine cervix. J Nucl Med 2008; 49: 1177-82.

[76] Dietz DW, Dehdashti F, Grigsby PW, Malyapa RS, Myerson RJ, Picus J, Ritter J, Lewis JS, Welch MJ, Siegel BA. Tumor hypoxia detected by positron emission tomography with 60Cu-ATSM as a predictor of response and survival in patients undergoing Neoadjuvant chemoradiotherapy for rectal carcinoma: a pilot study. Dis Colon Rectum 2008; 51: 1641-8.

[77] Vavere AL, Lewis JS. Cu-ATSM: A radiopharmaceutical for the PET imaging of hypoxia. Dalton Transactions 2007; 4: 4893-4902.

[78] Tateichi K, Tateishi U, Sato M, Yamanaka S, Kanno H, Murata H, Inoue T, Kawahara N. Application of 62Cu-diacetyl-bis(N4-methylthiosemicarbazone) PET imaging to predict highly malignant tumor grades and hypoxia-inducible factor-1a expression in patients with glioma. AJNR Am J Neuroradiol 2013; 34: 92-9.

[79] Lawrentschuk N, Lee FT, Jones G, Rigopoulos A, Mountain A, O'Keefe G, Papenfuss AT, Bolton DM, Davis ID, Scott AM. Investigation of hypoxia and carbonic anhydrase IX expression in a renal cell carcinoma xenograft model with oxygen tension measurements and 124I-cG250 PET/CT. Urol Oncol 2011; 29: 411-420.

[80] van Dijk J, Uemura H, Beniers AJ, Peelen WP, Zegveld ST, Fleuren GJ, Warnaar SO, Oosterwijk E. Therapeutic effects of monoclonal antibody G250, interferons and tumor necrosis factor, in mice with renal-cell carcinoma xenografts. Int J Cancer 1994; 56: 262-268.

[81] Hoeben BAW, Kaanders JHAM, Franssen GM, Troost EG, Rijken PF, Oosterwijk E, van Dongen GA, Oyen WJ, Boerman OC, Bussink J. PET of Hypoxia with 89Zr-labeled cG250-F(ab')2 in Head and Neck tumours. J Nucl Med 2010; 51: 1076-1083.

[82] Jerabek PA, Patrick TB, Kilbourn MR, Dischino DD, Welch MJ. Synthesis and biodistribution of of ^{18}F-labeled fluoronitroimidazoles: potential in vivo markers of hypoxic tissue. Int J Radiat Appl Instrum Part A 1986; 37: 599-605.

[83] Grierson JR, Link JM, Mathis CA, Rasey JS, Krohn KA. Radiosynthesis of fluorine-18 fluoromisonidazole. J Nucl Med 1989; 30: 343-50.

[84] Hoigebazar L, Jeong JM. Hypoxia imaging agents labeled with positron emitters. Recent Results cancer Res 2013; 194: 285-99.

[85] Takasawa M, Moustafa RR, Baron JC. Applications of Nitromidazole in vito hypoxia imaging in ischemic stroke. Stroke 2008; 39: 1629-37.

[86] Troost EGC, Laverman P, Kaanders JHAM, Philippens M, Lok J, Oyen WJG, van der Kogel, Boermann OC, Bussink J. Imaging hypoxia after oxygenation modification: comparing [18F] FMISO autoradiography with pimonidazole immunohistochemistry in human xenograft tumors. Radiother Oncol 2006; 80: 157-64.

[87] Troost EGC, Laverman P, Philippens MEP, Lok J, van der Kogel AJ, Oyen WJG, Boerman OC, Kaanders JH, Bussink J. Correlation of [18F] FMISO autoradiography and pimonidazole immunohistochemistry in human head and neck carcinoma xenografts. Eur J Nucl Med Mol Imaging 2008; 35: 1803-11.

[88] Arabi M, Piert M. Hypoxia PET/CT imaging: implications for radiation oncology. Q J Nucl Med Mol Imaging 2010; 54: 500-9.

[89] Thorwarth D, Alber M. Implementation of hypoxia imaging into treatment planning and delivery. Radiother Oncol 2010; 97: 172-175.

[90] Carlin S, Zhang H, Reese M, Ramos NN, Chen Q, Ricketts SA. A comparison of the imaging characteristics and microregional distribution of 4 hypoxia PET tracers. J Nucl Med 2014; 55: 515-21.

[91] Valk PE, Mathis CA, Prados MD, Gilbert JC, Budinger TF. Hypoxia in human gliomas: demonstration by PET with fluorine-18-fluoromisonidazole. J Nucl Med 1992; 33: 2133-7.

[92] Swanson KR, Chakraborty G, Wang CH, Rockne R, Harpold HLP, Muzi M, Adamsen TCH, Kenneth AK, Spence AM. Complementary but distinct role for MRI and 18F-fluoromisonidazole PET in the assessment of human glioblastomas. J Nucl Med 2009; 50: 36-44.

[93] Kawai N, Maeda Y, Kudomi N, Miyake K, Okada M, Yamamoto Y, Nishiyama Y, Tamiya T. Correlation of biological aggressiveness assessed by 11C-methionie PET and hypoxic burden assessed by 18F-fluoromisonidazole PET in newly diagnosed glioblastoma. Eur J Nucl Med Mol Imaging 2011; 38: 441-450.

[94] Rischin D, Hicks RJ, Fisher R, Binns D, Corry J, Porceddu S, Peters LJ. Prognostic significance of [18F]-misonidazole positron emission tomography-detected tumor hypoxia in patients with advanced head and neck cancer randomly assigned to chemoradiation with or without tirapazamine: a substudy of Trans-Tasman Radiation Oncology Group Study 98.02. J Clin Oncol 2006; 24: 2098-104.

[95] Nehmeh SA, Schoder H, Lee NY, Squire O, Zanzonico PB, Erdi YE, Greco C, Mageras G, Pham HS, Larson SM, Ling CC, Humm JL. Reproducibility of the intra-tumoral distribution of 18F-flouromisonidazole (18FMISO) in head and neck cancer. Int J Radiat Oncol Biol Phys 2008; 70: 235-242.

[96] Lin Z, Mechalakos J, Nehmeh S, Schoder H, Lee N, Humm J, Ling CC. The influence of changes in tumor hypoxia on dose-painting treatment plans based on 18F-FMISO positron emission tomography. Int J Radiation Oncology Biol Phys 2008; 70: 1219-28.

[97] Roels S, Slagmolen P, Nuyts J, Lee JA, Loeckx D, Maes F, Stroobants S, Penninckx F, Haustermans K. Biological image-guided radiotherapy in rectal cancer: is there a role for FMISO or FLT, next to FDG? Acta Oncol 2008; 48: 1237-48.

[98] Okamoto Sh, Shiga T, Yasuda K, Ito YM, Magota K, Kasai K, Kuge Y, Shirato H, Tamaki N. High reproducibility of tumor hypoxia evaluated by 18F-FMISO PET for head and neck cancer. J Nucl Med 2013; 54: 201-7.

[99] Tachibana I, Nishimura Y, Shibata T, Kanamori S, Nakamatsu K, Koike R, Nishikawa T, Ishikawa K, Tamura M, Hosono M. A prospective clinical trial of tumor hypoxia imaging with 18F-fluoromisonidazole positron emission tomography and computed tomography (F-MISO PET/CT) before and during radiation therapy. J Radiat Res 2013; 54: 1078-84.

[100] Lee N, Nehmeh S, Schoder H, Fury M, Chan K, Ling C, Humm J. Prospective trial incorporating pre-/mid-treatment [18F]-misonidazole positron emission tomography for head-and-neck

cancer patients undergoing concurrent chemoradiotherapy. Int J Radiation Oncology Biol Phys 2009; 75: 101-8.
[101] Hugonnet F, Fournier L, Medioni J, Smadja C, Hindie E, Huchet V, Itti E, Cuenod CA, Chantellier G, Oudard S, Faraggi M. Metastastic renal cell carcinoma: relationship between initial metastatic hypoxia, change after 1 month's sunitinib and therapeutic response: an 18F-fluoromisonidazole PET/CT study. J Nucl Med 2011; 52: 1048-55.
[102] Kumar P, Stypinski D, Xia H, McEwan AJB, Machulla HJ, Wiebe LI. Fluoroazomycin arabinoside (FAZA): Synthesis, H-2 and H-3-labelling and preliminary biological evaluation of a novel 2-nitroimidazole marker of tissue hypoxia. J Label Compd Radiopharm 1999; 42: 3-16.
[103] Busk M, Horsman MR, Jakobsen S, Bussink J, van der Kogel A, Overgaard J. Cellular uptake of PET tracers of glucose metabolism and hypoxia and their linkage. Eur J Nucl Med Mol Imaging 2008; 35: 2294-2303.
[104] Piert M, Machulla HJ, Picchio M, Reischl G, Ziegler S, Kumar P, Wester HJ, Beck R, McEwan AJ, Wiebe LI, Schawaiger M. Hypoxia-specific tumour imaging with 18F-fluoroazomycin arabinoside. J Nucl Med 2005; 46: 106-13.
[105] Busk M, Munk OL, Jakobsen S, Wang T, Skals M, Steiniche T, Horsman MR, Overgaard J. Assessing hypoxia in animal tumor modls based on pharmacokinetic analysis of dynamic FAZA PET. Acta Oncol 2010; 49: 922-33.
[106] Shi K, Souvatzoglou M, Astner ST, Vaupel P, Nusslin F, Wilkens JJ, Ziegler SI. Quantitative assessment of hypoxia kinetic models by cross-study of dynamic 18F-FAZA and 150-H20 in patients with head and neck tumors. J Nucl Med 2010; 51: 1386-94.
[107] Halmos GB, de Bruin LB, Langendijk JA, van der Laan BF, Pruim J, Steenbakkers RJ. Head and neck hypoxia imaging by 18F-fluoroazomycin-arabinozide (18F-FAZA)-PET: a review. Clin Nucl Med 2014; 39: 44-8.
[108] Sorger D, Patt M, Kumar P, Wiebe LI, Barthel H, Seese A, Dannenberg C, Tannapfel A, Kluge R, Sabri O. [18F]-Fluoroazomycin arabinofuranoside (18FAZA) and [18F]-Fluoromisonidazole (18FMISO): a comparative study of their selective uptake in hypoxic cells and PET imaging in experimental rat tumours. Nucl Med Biol 2003; 30: 317-26.
[109] Beck R, Röper B, Carlsen JM, Huisman MC, Lebschi JA, Andratschke N, Picchio M, Souvatzoglou M, Machulla HJ, Piert M. Pretreatment 18F-FAZA PET predicts success of hypoxia-directed radiochemotherapy using tirapazamine. J Nucl Med 2007; 48: 973-80
[110] Maier FC, Kneiling M, Reischl G, Cay F, Bukala D, Schimd A, Judenhofer MS, Rocken M, Machulla H, Pichler BJ. Significant impact of different oxygen breathing conditions on noninvasive in vivo tumor-hypoxia imaging using [18F]-fluoro-azomycinarabino-furanoside ([18F]FAZA). Radiat Oncol 2011; 6: 165.
[111] Tran LBA, Bol A, Labar D, Jordan B, Magat J, Mignion L, Gregoire V, Gallez B. Hypoxia imaging with the nitroimidazole 18F-FAZA PET tracer: a comparison with OxyLite, EPR oximetry and 19F-MRI relaxometry. Radiother Oncol 2012; 105: 29-35.
[112] Busk M, Mortensen LS, Nordmark M, Overgaard J, Jakobsen S, Hansen KV, Theil J, Kallehauge JF, D'Andrea FP, Steiniche T, Horsman MR. PET hypoxia imaging with FAZA: reproducibility at baseline and during fractionated radiotherapy in tumour-bearing mice. Eur J Nucl Med Mol Imaging 2013; 40: 186-197.
[113] Solomon B, Binns D, Roselt P, Weibe LI, McArthur GA, Cillinane C, Hicks RJ. Modulation of intratumoral hypoxia by epidermal growth factor receptor inhibitor gefitinib detected sging small animal PET imaging. Mol Cancer Ther 2005; 4: 1417-22.
[114] Mortensen LS, Busk M, Nordsmark M, Jakobsen S, Theil J, Overgaard J, Horsman MR. Accessing radiation response using hypoxia PET imaging and oxygen sensitive electrodes: a preclinical study. Radiother Oncol 2011; 99: 418-423.
[115] Postema EJ, McEwan AJB, Riauka TA, Kumar P, Richmond DA, Abrams DN, Wiebe LI. Initial results of hypoxia imaging using 1-a´-D-(5-deoxy-5-[18F]-fluoroarabinofuranosyl)-2-nitroimidazole (18F-FAZA). Eur J NuclMed Mol Imaging 2009; 36: 1565.
[116] Grosu AL, Souvatzoglou M, Roper B, Dobritz M, Wiedenmann N, Jacob V, Wester HJ, Reischl G, Machulla HJ, Schwaiger M, Molls M, Piert M. Hypoxia imaging with FAZA-PET and theoretical considerations with regard to dose painting for individualization of radiotherapy in patients with head and neck cancer. Int J Radiat Oncol Biol Phys 2007; 69: 541-551.
[117] Yang DJ, Wallace S, Cherif A, Li C, Gretzer MB, Kim EE, Podoloff DA. Development of F-18-labeled fluoroerythronitroimidazole as a PET agent for imaging tumor hypoxia. Radiology 1995; 194: 795-800.
[118] Lehtiö K, Eskola O, Viljanen T, Oikonen V, Groenroos T, Sillanmaeki L, Grenman R, Minn H. Imaging perfusion and hypoxia with PET to predict radiotherapy response in head-and-neck cancer. Int J Radiat Oncol Biol Phys 2004; 59: 971-82.
[119] Grönroos T, Bentzen L, Marjamäki P, Murata R, Horsman MR, Keiding S, Eskola O, Haaparanta M, Minn H, Solin O. Comparison of the biodistribution of two hypoxia markers [18F]FETNIM

and [18F]FMISO in an experimental mammary carcinoma. Eur J Nucl Med Mol Imaging 2004; 31: 513-20.
[120] Laughlin KM, Evans SM, Jenkins WT, Tracy M, Chan CY, Lord EM, Koch CJ. Biodistribution of the nitroimidazole EF5 (2-[2-nitro-1H-imidazol-1-yl]-N-(2,2,3,3,3-pentafluoropropyl) acetamide) in mice bearing subcutaneous EMT6 tumors. J Pharmacol Exp Ther 1996; 277: 1049-1057.
[121] Josse O, Labar D, georges B, Gregoire V, Marchand-Brynaert J. Synthesis of [18F]-labeled EF3 [2-(2-Nitroimidazol-1yl)-N-(3,3,3-trifluoropropyl)-acetamide], a Marker fro PET Detection of Hypoxia. Bioorg Med Chem 2001; 9: 665-75.
[122] Fujibayashi Y, Taniuchi H, Yonekura Y, Ohtani H, Konishi J, Yokoyama A. Copper-62-ATSM: A new hypoxia imaging agent with high membrane permeability and low redox potential. J Nucl Med 1997; 38: 1155-60.
[123] Hustinx R, Eck SL, Alavi A. Potential Applications of PET Imaging in Developing Novel Cancer Therapies. J Nucl Med 1999; 40: 995-1002.
[124] Chen K, Che X. Positron Emission Tomography Imaging of Cancer Biology: Current Status and Future Prospects. Semin Oncol 2011; 38: 70-86.
[125] Dealing JLJ, Lewis JS, McCarthy DW, Welch MJ, Blower PJ. Redox-active metal complexes for imaging hypoxic tissues: structure-activity relationships in cooper(II)bis(thiosemicarbazone) complexes. Chem Commun (Camb) 1998; 22: 2531-2.
[126] Lewis JS, McCarthy DW, McCarthy TJ, Fujibayashi Y, Welch MJ. Evaluation of 64Cu-ATSM in vitro and in vivo in hypoxic tumor model. J Nucl Med 1999; 40: 177-83.
[127] Hueting R, Kersemans V, Cornelissen B, Tredwell M, Hussein K, Christlieb M, Gee AD, Passchier J, Smart SC, Dilworth JR, Gouverneur V, Muschel RJ. A comparison of the behavior of 64Cu-Acetate and 64Cu-ATSM in vitro and in vivo. J Nucl Med 2014; 55: 128-34.
[128] Takahashi N, Fujibayashi Y, Yonekura Y, Welch MJ, Waki A, Tsuchida T, Sadato N, Sugimoto K, Itoh H. Evaluation of 62Cu labeled diacetyl-bis(N4-methylthiosemicarbazone) as a hypoxic tissue tracer in patients with lung cancer. Ann Nucl Med 2000; 14: 323-8.
[129] Dehdashti F, Grigsby PW, Lweis JS, Laforest R, Siegel BA, Welcj MJ. Assessing tumor hypoxia in cervical cancer by PET with 60Cu-labeled diacetyl-bis(N4-methylthiosemicarbazone). J Nucl Med 2008; 49: 201-5.
[130] Yuan H, Schroeder Th, Bowsher JE, Hedlund LW, Wong T, Dewhirst MW. Intertumoral differences in hypoxia selectivity of the PET imaging agent 64Cu(II)-diacetyl-bis(N4-methylthiosemicarbazone). J Nucl Med 2006; 47: 989-98.
[131] Vavere AL, Lewis JS. Examining the relationship between Cu-ATSM hypoxia selectivity and fatty acid synthase expression in human prostate cancer cell lines. Nucl Med Biol 2008; 35: 273-279.
[132] O'Donoghue J, Zanzonico P, Pugachev A, Wen B, Smith-Jones P, Cai Sh, Burnazi E, Finn R, Burgman P, Ruan Sh, Lewis JS, Welch MJ, Ling CC, Humm JL. Comparative study featuring microPET imaging, Po2 probe measurement, autoradiography, and frlurescent microscopy in the R3327-AT and FaDu rat tumor models. Int J Radiat Oncol Biol Phys 2005; 61: 1493-1502.
[133] Jalilian AR, Rostampour N, Rowshanfarzad P, Shafaii K, Kamali-Dehghan M, Akhlaghi M. Preclinical studies of [61Cu]ATSM as a PET radiopharmaceutical for fibrosarcoma imaging. Acta Pharm 2009; 59: 45-55.
[134] Dalah E, Bradley D, Nisbet A. Simulation of tissue activity curves of 64Cu-ATSM for sub-target volume delineation in radiotherapy. Phys Med Biol 2010; 55: 681-694.
[135] Chao KS, Bosch WR, Mutic S, Lewis JS, Dehdashti F, Mintum MA, Dempsey JF, Perez CA, Purdy JA, Welch MJ. A novel approach to overcome hypoxic tumor resistance: Cu-ATSM-guided intensity modulated radiation therapy. Int J Radiat Oncol Biol Phys 2001; 49: 1171-1182.
[136] Laforest R, Dehdashti F, Lewis JS, Schwarz SW. Dosimetry of 60/61/62/64Cu-ATSM: a hypoxia imaging agent for PET. Eur J Nucl Med Mol Imaging 2005; 32: 764-70.
[137] McCarthy DW, Bass LA, Cutler PD, Shefer RE, Klinkowstein RE, Herrero P, Lewis JS, Cutler CS, Anderson CJ, Welch MJ. High purity production and potential applications of copper-60 and copper-61. Nucl Med Biol 1999; 26: 351-358.
[138] http://www.nndc.bnl.gov/nudat2/ NuDat 2 is a software product that allows to search and plot nuclear structure and nuclear decay data interactively. NuDat 2 was developed by the National Nuclear Data Center (NNDC) in Brookhaven National Laboratory.
[139] Partridgea M, Spinelli, A, Rydera W, Hindorfa C. The effect of β+ energy on performance of a small animal PET camera. Nuclear Instruments and Methods in Physics Research Section A: Accelerators, Spectrometers, Detectors and Associated Equipment 2006; 568: 933-6.
[140] Blower PJ, Lewis JS, Zweit J. Copper radionuclides and radiopharmaceuticals in nuclear medicine. Nuclear Medicine and Biology 1996; 23: 927-1025.
[141] Weeks AJ, Paul RL, Marsden PK, Blower PJ, Lloyd DR. Radiobiological effects of hypoxia-

dependent uptake of 64Cu-ATSM: enhanced DNA damage and cytotoxicity in hypoxic cells. Eur J Nucl Med Mol Imaging 2010; 37: 330-8.
[142] Lewis J, Laforest R, Buettner T, Song S, Fujibayashi Y, Connett J, Welch M. Copper-64-diacetyl-bis(N4-methylthiosemicarbazone): an agent for radiotherapy. Proc Natl Acad Sci U S A 2001; 98: 1206-11.
[143] Yoshii Y, Furukawa T, Kiyono Y, Watanabe R, Mori T, Yoshii H, Asai T, Okazawa H, Welch MJ, Fujibayashi Y. Internal radiotherapy with copper-64-diacetyl-bis(N4-methylthiosemicarbazone) reduces CD133+ highly tumorigenic cells and metastatic ability of mouse colon carcinoma. Nucl Med Biol 2011; 38: 151-57.
[144] Gatenby RA, Gawlinski ET. A reaction-diffusion model of cancer invasion. Cancer Res 1996; 56: 5745-5753.
[145] Shuch B, Li Z, Belldegrun AS. Carbonic anhydrase IX and renal cell carcinoma: Prognosis, response to systemic therapy, and future vaccine strategies. BJU Int 2008; 101 Suppl 4: 25-30.
[146] Oosterwijk E, Ruiter DJ, Hoedemaeker PJ, Pauwels EK, Jonas U, Zwartendijk J, Warnaar SO. Monoclonal antibody G250 recognizes a determinant present in renal cell carcinoma and absent from normal kidney. Int J Cancer 1986; 38: 489-494.
[147] Divgi CR, Pandit-Taskar N, Jungbluth AA, Reuter VE, Gönen M, Ruan S, Pierre C, Nagel A, Pryma DA, Humm J, Larson SM, Old LJ, Russo P. Preoperative characterisation of clear-cell renal carcinoma using iodine-124-labelled antibody chimeric G250 (^{124}I-cG250) and PET in patients with renal masses: a phase I trial. Lancet Oncol 2007; 8: 304-310.